The Journal of Immunology

Expression and Activity of NOX5 in the Circulating Malignant B Cells of Hairy Cell Leukemia

Aura S. Kamiguti, Lena Serrander, Ke Lin, Robert J. Harris, John C. Cawley, David J. Allsup, Joseph R. Slupsky, Karl-Heinz Krause and Mirko Zuzel

J Immunol 2005; 175:8424-8430; ;
doi: 10.4049/jimmunol.175.12.8424
http://www.jimmunol.org/content/175/12/8424

The Journal of Immunology is published twice each month by
The American Association of Immunologists, Inc.,
1451 Rockville Pike, Suite 650, Rockville, MD 20852

Print ISSN: 0022-1767 Online ISSN: 1550-6606.

Expression and Activity of NOX5 in the Circulating Malignant B Cells of Hairy Cell Leukemia[1]

Aura S. Kamiguti,[2]* Lena Serrander,† Ke Lin,* Robert J. Harris,* John C. Cawley,* David J. Allsup,* Joseph R. Slupsky,* Karl-Heinz Krause,† and Mirko Zuzel*

Hairy cells (HCs) are mature malignant B cells that contain a number of constitutively active signaling molecules including GTP-bound Rac1, protein kinase C, and Src family kinases. Because Rac1 is a component of the reactive oxidant species (ROS)-generating NADPH oxidase system, we investigated the role of this GTPase in ROS production in HCs. In this study, we show that ROS production in HCs involves a flavin-containing oxidase dependent on Ca^{2+}, but not on GTP-Rac1 or protein kinase C. This suggests the involvement of the nonphagocytic NADPH oxidase NOX5, an enzyme found in lymphoid tissues, but not in circulating lymphocytes. By using RT-PCR and Southern and Western blotting and by measuring superoxide anion production in membrane fractions in the absence of cytosolic components, we demonstrate for the first time that HCs (but not circulating normal B cells or some other lymphoid cell types) express NOX5. We also demonstrate that inhibition of NADPH oxidase in HCs results in a selective increase in the activity of Src homology region 2 domain-containing phosphatase 1 (SHP-1). Furthermore, SHP-1 in HCs coimmunoprecipitates with tyrosine phosphorylated CD22 and localizes in the same cellular compartment as NOX5. This allows the inactivation of SHP-1 by NOX5-generated ROS and contributes to the maintenance of the constitutive activation of HCs. ***The Journal of Immunology,*** **2005, 175: 8424–8430.**

Hairy cell (HC)[3] leukemia (HCL) is a chronic B cell malignancy characterized by the presence in the circulation of pathognomonic HCs. A prominent feature of these cells is the presence of distinctive surface projections or hairs which gave the disease its name. It is now generally accepted that HCs are clonal late B cells with specific features of activation (1). Whether or not HCs have a normal counterpart and the nature of the underlying oncogenic event(s) remain unknown. Specific features of activation include elevated cytosolic Ca^{2+} levels (2) and activation of both Src kinases (3) and the Rho GTPases Rac1 and Cdc42 (4). In addition, we have recently demonstrated the important role of both protein kinase C (PKCs) and Src in the constitutive activation of MAP kinases in HCs (5).

Because both Rac1 and PKC play a central role in the activation of NADPH oxidase in many cell types (6, 7), we have examined reactive oxidant species (ROS) production by HCs, the role of Rac1 and PKCs in this process, and the effect of ROS on constitutive HC signaling.

Our results showed that the production of ROS in HCs is Rac1- and PKC-independent, but Ca^{2+}-dependent and sensitive to diphenyleneiodonium (DPI; an inhibitor of flavin-containing oxidases), suggesting involvement of the nonphagocytic oxidase, NOX5 (8). NOX5, a membrane-associated homolog of the $gp91^{phox}$ subunit of NADPH oxidase (9), is selectively expressed in testis, spleen, and lymph nodes (10), but absent from circulating lymphocytes (11). In this study, we demonstrate that both NOX5 protein and message are indeed expressed by HCs, but are largely absent from the malignant cells of chronic lymphocytic leukemia (CLL), marginal-zone leukemia (MZL), and mantle-cell leukemia (MCL) and from normal peripheral blood B cells. Because ROS inhibit protein tyrosine phosphatases (PTPs) by oxidizing the sulfydryl group in the catalytic pocket of these enzymes (12–14), we also examined whether NOX5-produced oxidants have this effect in HCs. We showed that NOX5 colocalizes with Src homology region 2 domain-containing phosphatase 1 (SHP-1) and plays an important role in the regulation of this PTP, an enzyme central to the negative regulation of protein tyrosine phosphorylation-dependent activation of B cells.

To our knowledge, the present study represents the first demonstration of the expression and specific function of NOX5 in a circulating, albeit malignant, lymphoid cell type.

Materials and Methods

Cells

Experiments were conducted using primary malignant cells obtained from HCL, CLL, MZL, and MCL leukemia patients. Material was obtained with informed consent and with the approval of the Liverpool Research Ethics Committee. Malignant cells were purified by negative depletion of T cells and monocytes, but were also studied without such depletion. Negative depletion had no effect on the expression of either NOX5 protein or message (Fig. 3*E*). Normal B cells were purified either negatively as above or positively with CD19-coated beads. No NOX5 protein or message was detectable in the normal circulating B cells, regardless of the method of purification. Polymorphonuclear cells (PMN) were isolated from normal blood as described (15). Before use, cell suspensions in RPMI 1640 medium containing 1 mg/ml BSA, 2 mM L-glutamine, 100 U/ml penicillin, and 100 μg/ml streptomycin were left for 60 min in a CO_2 incubator at 37°C to allow cells to recover from the various centrifugation steps during

*Department of Hematology, Royal Liverpool Hospital, University of Liverpool, Liverpool, United Kingdom; and †Department of Geriatrics, University Hospital of Geneva, Geneva, Switzerland

Received for publication May 17, 2005. Accepted for publication September 29, 2005.

The costs of publication of this article were defrayed in part by the payment of page charges. This article must therefore be hereby marked *advertisement* in accordance with 18 U.S.C. Section 1734 solely to indicate this fact.

[1] This work was supported by the Leukaemia Research Fund U.K.

[2] Address correspondence and reprint requests to Dr. Aura S. Kamiguti, Department of Hematology, Royal Liverpool Hospital, University of Liverpool, Daulby Street, Liverpool L69 3GA, United Kingdom. E-mail address: aurakami@liverpool.ac.uk

[3] Abbreviations used in this paper: HC, hairy cell; HCL, HC leukemia; ROS, reactive oxidant species; DPI, diphenyleneiodonium; DCF-DA, 2′,7′-dichlorodihydrofluorescein diacetate; CLL, chronic lymphocytic leukemia; MZL, marginal-zone leukemia; MCL, mantle-cell leukemia; PMN, polymorphonuclear cell; PTP, protein tyrosine phosphatase; pNPP, *p*-nitrophenyl phosphate; SHP-1, Src homology region 2 domain-containing phosphatase 1; SOD, superoxide dismutase.

0022-1767/05/$02.00

purification. To avoid adhesion, all B cell cultures were in polyHEMA-coated tissue culture plates. The HEK293 cell line transfected with NOX5 (10) was used as positive control.

Reagents

p-Nitrophenyl phosphate (pNPP), PMSF, DPI, FAD, phosphatidic acid (1,2 didecanoyl-*sn*-glycerol-3-phosphate), cytochrome *c* (bovine heart), NADPH, superoxide dismutase (SOD), fibronectin, leupeptin, and cell culture grade BSA were purchased from Sigma-Aldrich. GM-CSF was from R&D Systems Europe. Aprotinin was obtained from Bayer, tissue culture medium and Lymphoprep were from Invitrogen Life Technologies, and protein G-Sepharose was from Zymed Laboratories. 2′,7′-Dichlorodihydrofluorescein diacetate (DCF-DA) was from Molecular Probes. Reagents for protein determination were purchased from Bio-Rad. Polyvinylidene difluoride (Immobilon-P) membrane from Millipore, and ECL reagent and Hyperfilm from Amersham Pharmacia were also used. PKC inhibitor Ro-32-0432, Rho-GTPase family inhibitor from *Clostridium difficile*, toxin B, and BAPTA-AM were from Calbiochem-Novabiochem. Purified vitronectin was prepared from human serum as described before (16). All other reagents used were of analytical grade.

Antibodies

Polyclonal Ab against NOX5-EF hand motifs was produced in rabbits as described before (8). Rabbit polyclonal Abs against SHP-1, SHP-2, and p56/p53 Lyn were obtained from Santa Cruz Biotechnology. Abs against PTP-1B and Rac1 were from Upstate Biotechnology. mAb anti-β-actin was purchased from Sigma-Aldrich, anti-phosphotyrosine (PY20) was from Transduction Laboratories, and anti-SHP-1 and anti-CD22 were both from BD Biosciences.

RT-PCR

RNA extracts from cells (1 μg) were reverse transcribed with Moloney murine leukemia virus reverse transcriptase (Promega) and an oligo$(dT)_{15}$ primer. The resulting cDNAs were used as template to amplify *nox5* transcripts in a 50-μl reaction containing 0.4 μM forward primer (5′-GTGC TACATCGATGGGCCTTATG-3′) and reverse primer (5′-CCCCGT GATGGAGTCTTTCTTCT-3′), 1.5 mM $MgCl_2$, 200 μM of each dNTP, and 2.5 U of *Taq*DNA polymerase in supplied buffer from Promega. The 2-min initial denaturation at 94°C was followed by 38 cycles of PCR, each consisting of 30 s denaturation at 94°C, 30 s annealing at 65°C, and 60 s extension at 72°C. The PCR finished after a further 7-min extension. Under similar conditions, *gapdh* and *β-actin* were both amplified as internal controls for each cDNA using a pair of primers for the former (forward, 5′-AGCCA CATCGCTCAGACACC-3′ and reverse, 5′-GTACTCAGCGCCAGCAT CG-3′) and for the latter (forward, 5′-CCTCGCCTTTGCCGATCC-3′and reverse, 5′-GATCTTCATGAGGTAGTCAGTC-3′).

Southern blot analysis

nox5 RT-PCR products were size-fractionated on a 1.8% agarose gel and transferred onto a nylon membrane. The membrane was subsequently hybridized with ^{32}P-labeled *nox5* probe, which had been gel-purified and subcloned in a pGEM-Teasy vector (Promega). The probe was shown by sequencing to be a 433-bp fraction of *nox5* cDNA (GenBank accession number AF325190). After washing, the membrane was subjected to autoradiography. *β-Actin*, as template control, was amplified with PCR from each cDNA sample and stained with ethidium bromide.

Rac1 pull-down assay

A plasmid clone, pGEX-PAK, encoding a GST-p21-activated protein kinase binding domain (Cdc42-/Rac1-binding domain, aa 59–272) fusion protein, designated GST-PBD, was a generous gift from Prof. A. Hall (University College London, London, U.K.). pGEX-PAK was expressed in *Escherichia coli,* and the GST-PBD fusion protein was purified as described (17). A total of 10^7 cells were lysed (25 mM Tris-HCl (pH 7.5) lysis buffer containing 5 mM $MgCl_2$, 1% Nonidet P-40, 5% glycerol, 1 mM PMSF, 1 μg/ml leupeptin, 1 μg/ml aprotinin, and 1 mM sodium vanadate) in the presence of 8 μg of GST-PBD. Proteins bound to GST-PBD were isolated by affinity precipitation onto glutathione-Sepharose 4B beads and analyzed in a 12% gel by SDS-PAGE followed by Western blotting.

Immunoprecipitation and Western blotting analysis

Preparation of cell lysates and of immunoprecipitates, SDS-PAGE, and Western blotting were conducted as described before (5). The intensity of the bands was analyzed by densitometry.

Measurement of ROS production by fluorescence

To measure ROS production, cells (10^6/ml) were incubated with 10 μM DCF-DA for 30 min at 37°C. DCF-DA is a cell-permeable, nonfluorescent probe that is oxidized by ROS to produce dichlorofluorescein. After incubation, cells were washed once with PBS, and the intensity of the fluorochrome measured by flow cytometry (BD Biosciences).

Measurement of superoxide generation in cell-free systems

Membrane and cytosolic fractions were prepared by lysing HCs (2×10^7) in 1 ml of ice-cold sucrose buffer (10 mM Na_2HPO_4 (pH 7.4), 140 mM NaCl, 340 mM sucrose, 2 mM sodium azide, 1 mM EGTA, 1 mM PMSF, 1 μg/ml leupeptin, and 1 μg/ml pepstatin) followed by sonication (15 s at 30% duty cycle). Cell lysates were centrifuged (4°C) first at $10,000 \times g$ for 10 min to sediment nuclei and mitochondria. The supernatants were then centrifuged at $100,000 \times g$ for 60 min, the cytosol was preserved, and the membrane pellets were resuspended in 100 μl of sucrose buffer. Protein concentration of cytosol and membrane preparations was determined. Assays for superoxide production were conducted in duplicate in reaction mixtures (100 μl) containing 10 μg of membrane protein with or without 30 μg of cytosolic proteins and 10 μM FAD, 1 mM $MgCl_2$, 1 mM $CaCl_2$, 5.5 μM phosphatidic acid, and 100 μM cytochrome *c*, in PBS (pH 7.5). Parallel duplicate samples were prepared with or without addition of 400 U/ml SOD. Superoxide anion production was initiated by adding 200 μM NADPH and followed for 20 min. Superoxide generation was determined from the rate of SOD-inhibitable reduction of cytochrome *c* measured at 550 nm (18). The absorption coefficient of reduced cytochrome *c* (21 $mM^{-1} \cdot cm^{-1}$) was used for calculation of the amount of superoxide produced.

Protein tyrosine phosphatase (PTP) assay

Cells (5×10^6) were lysed in cold PTP lysis buffer (1% Nonidet P-40 in 10 mM HEPES (pH 7.6) containing 15 mM KCl, 2 mM $MgCl_2$, 1 mM PMSF, 1 μg/ml leupeptin, and 1 μg/ml aprotinin). SHP-1, SHP-2, and PTP-1B were immunoprecipitated from the lysates with respective Abs bound to protein G-Sepharose beads. Blanks containing lysis buffer only were processed in the same way. Beads were washed and resuspended in 100 μl of PTP assay buffer (25 mM imidazol (pH 7.2), containing 45 mM NaCl and 1 mM EDTA) containing 1.5 mg/ml pNPP as substrate. After a 30-min incubation of the immunoprecipitates with the substrate at 37°C, reaction was stopped with addition of 20 μl of 13% K_2HPO_4, and the absorbances at 405 nm of supernatants were recorded against blank. PTP activity of whole cell lysates (5×10^5 cells) was also estimated. After the assay, beads were subjected to SDS-PAGE and Western blotting to detect immunoprecipitated phosphatase.

Isolation of lipid raft membrane fractions

Raft membranes were isolated from HCs (10^8 cells) using flotation on discontinuous Optiprep (Axis-Shield) density gradients (5–40%) as described (19). Cells were lysed for 30 min in 200 μl of ice-cold lysis buffer (10 mM Tris-HCl (pH 7.4), containing 150 mM NaCl, 1 mM EDTA, 0.5% Triton X-100, 1 mM Na_3VO_4, 1 mM PMSF, 1 μg/ml leupeptin, and aprotinin). The lysate was mixed with cold Optiprep to give a final 40% Optiprep concentration. The mixture was overlayed with 1 ml of 30% and 0.5 ml of 5% Optiprep in lysis buffer before being centrifuged at $250,000 \times g$ for 4 h at 4°C. Fractions of 150 μl were removed from the top to the bottom of the centrifuge tube. Fractions 3–5 (interface of 30 and 5% Optiprep) are lipid rafts, and fractions 10–12 (bottom) correspond to the nonraft membrane fractions. Then, 5 μg of each fraction was subjected to SDS-PAGE and Western blotting. Lyn (p56/p53) was used as a marker of lipid raft-containing fractions.

Statistical analysis

Statistical analysis was carried using paired-sample Student's *t* test, in which p values < 0.05 were considered to be significant.

Results

ROS production in HCs is independent of GTP-Rac1

Because HCs contain constitutively active Rac1 (4) and active PKCs (5), components known to be involved in the assembly of NADPH oxidase in several cell types (7, 20, 21), we first examined oxidant production in HCs. Unstimulated HCs loaded with DCF-DA produced intense fluorescence, which was measured at 1 h and persisted throughout a 24-h culture period in the absence of serum or cell adhesion (Fig. 1, control).

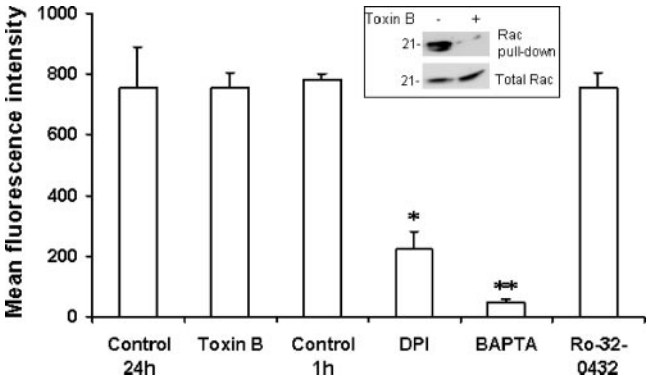

FIGURE 1. ROS production in HCs is dependent on an NADPH oxidase and intracellular Ca^{2+}, but independent of Rac1 and PKC. HCs (10^6/ml) were untreated (control) or treated with 20 ng/ml toxin B (24 h), 5 μM DPI (1 h), 10 μM BAPTA-AM (1 h), or 10 μM Ro-32-0432 (1 h). The fluorescence produced by oxidation of DCF-DA by ROS was measured by flow cytometry. Results are means ± SD of experiments conducted in three HCL cases. *, $p = 0.0055$ and **, $p = 0.0007$ vs control 1 h; paired-sample Student's *t* test. The *inset* shows a representative result of three independent experiments demonstrating the reduction of GTP-loaded Rac1 after HC treatment with toxin B.

To investigate the role of the constitutively active Rac1 in this process, cells were treated for up to 24 h with 20 ng/ml toxin B, a concentration that completely abolished the presence of GTP-Rac in HCs (Fig. 1, *inset*). This treatment did not affect constitutive ROS production (Fig. 1) and also had no effect on HC viability. Treatment with the general PKC inhibitor Ro-32-0432 (10 μM) for 1 h did not change ROS production (Fig. 1). In contrast, when cells were treated with 5 μM DPI (an NADPH oxidase inhibitor) or with 10 μM BAPTA-AM (an intracellular calcium chelator) for 1 h, there was a significant reduction in DCF fluorescence compared with that of control cells (Fig. 1). These results clearly demonstrate that ROS production in HCs is independent of GTP-Rac1 and PKC, but depends on a flavin-containing oxidase and Ca^{2+}.

Because the inhibition of ROS production by DPI suggested the involvement of an NADPH oxidase, we next examined whether cytosolic and cell membrane components were required for the assembly of the NADPH oxidase system. To do this, we measured DPI-sensitive superoxide anion production in membrane preparations and explored how this production is influenced by the addition of cytosolic proteins.

The membrane fraction of HCs produces superoxide anion

Fig. 2, *A* and *B* show that isolated plasma membrane preparations produced superoxide anion and that this production was not greatly altered by the addition of cytosolic proteins, but was strongly inhibited by DPI. This suggested that the membrane-associated enzyme did not require Rac1 or other cytosolic proteins for its activity. The lack of Rac1 involvement was then confirmed by the demonstration that the superoxide anion production by membranes of toxin B-treated HCs (at a concentration shown to inhibit GTPase-Rac1; Fig. 1, *inset*) did not differ from that of untreated cells (Fig. 2, *A* and *B*). This confirms the above results showing that active Rac1 does not participate in the activation of the DPI-sensitive oxidase in constitutively active HCs.

The dependence on Ca^{2+}, but not on Rac1 and PKC, led us to hypothesize that the enzyme responsible for the DPI-sensitive ROS production in HCs is NOX5. Because an increase in cytoplasmic Ca^{2+} level promotes activation of NOX5 (8), and because elevated levels of Ca^{2+} in HCs have already been reported (2, 22), this further strengthened our hypothesis that constitutive production of ROS in HCs involves NOX5. Therefore, we used Western blotting to examine the cells for the presence of NOX5 protein in subcellular fractions. We found that only the membrane fraction produced a band of ~70 kDa reactive with anti-NOX5 Ab (Fig. 2*C*).

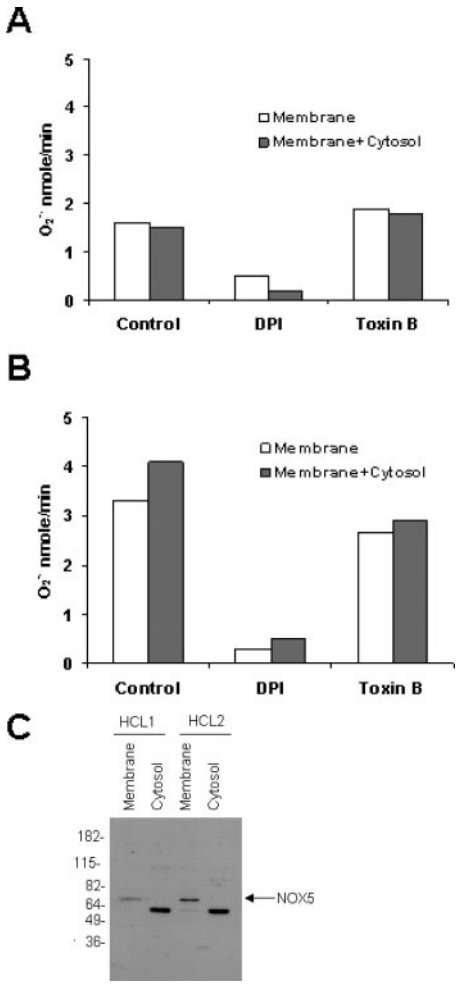

FIGURE 2. Isolated plasma-membrane fractions of HCs produce superoxide anion. O_2^- production was measured in reaction mixtures containing 10 μg of plasma-membrane protein with or without 30 μg of cytosolic proteins (see *Materials and Methods*). Superoxide anion production was initiated by adding 200 μM NADPH, and the rate of production was followed every 30 s for 20 min. *A* and *B,* The results in two cases in which the production was measured in preparations from control, 5 μM DPI-treated (60 min), or 20 ng/ml toxin B-treated (24 h) HCs. *C*, Western blots of membrane or cytosolic protein fractions (10 μg each) of cells from the two HCL patients using an anti-NOX5 Ab. Note that the band observed in the cytosolic fractions was not present in HEK293 control cells transfected with NOX5 (Fig. 3). Furthermore, the cytosol had negligible oxidase activity. Therefore, it seems likely that the smaller size band is a protein nonspecifically reacting with the anti-NOX5 Ab.

NOX5 is clearly expressed in HCs, but not in CLL or some other hemic cell types

Next, we again used Western blotting and demonstrated that all HCL clones examined express the ~70-kDa protein ($n = 10$; Figs. 3*A* and 4*A*). In contrast, the band could be barely detected in only one of the six CLL cases examined ($n = 6$; Fig. 3*C*, *lane 6*). The protein was also undetectable in both MZL ($n = 1$; Fig. 3*A*, *lane 6*) and MCL cells ($n = 3$; data not shown). NOX5 was also undetectable in normal peripheral blood B cells (Fig. 3*C*, *lanes*

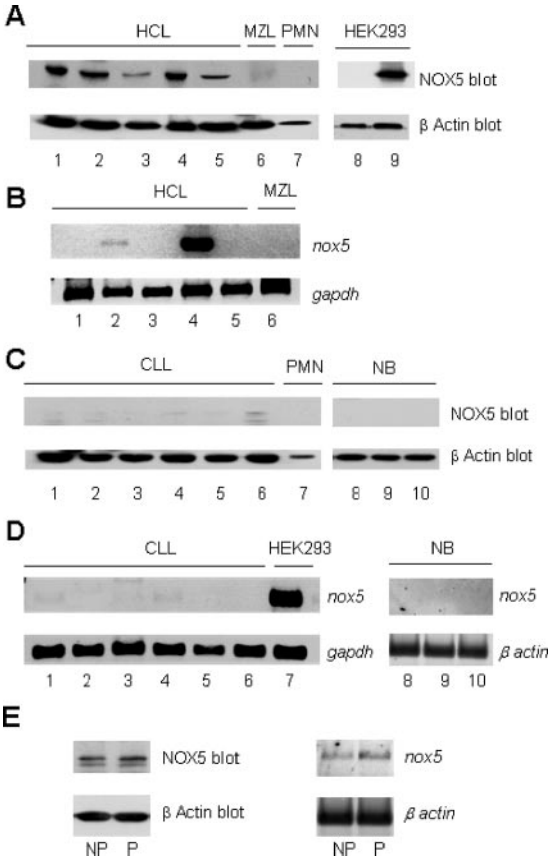

FIGURE 3. NOX5 is expressed in HCs but not in CLL cells. *A* and *C*, Western blots of lysates from 10^6 cells using an anti-NOX5 Ab. *A*, *Lanes 1–5* show the results with cells from five HCL cases; *lane 6* is an MZL cell lysate; *lane 7* is the PMN lysate from a normal donor and *lane 8* shows wild-type HEK293 cells, both used as negative controls; *lane 9* is the lysate of NOX5-transfected HEK293 cells used as a positive control. *C*, *Lanes 1–6* show the results with six CLL cases; *lane 7* is the negative control (PMN lysate); and *lanes 8–10* contain lysates of normal peripheral blood B (NB) cells. Blots of β-actin are shown as loading controls. *B* and *D*, RT-PCR results (negative images) of *nox5* and *gapdh* expression in HCL and CLL cells (*lanes 1–6*). *Lane 7* in *D* shows the result with NOX5-transfected HEK293 cells used as a positive control. *Lanes 8–10* in *D* show *nox5* and *β-actin* expression in normal peripheral blood B (NB) cells. *Left panels* in *E* show Western blotting of NOX5 and β-actin in HC lysates from nonpurified (NP) and purified (P) cells, and the *right panels* show the corresponding NOX5 RT-PCR results.

8–10). Lysates of PMN (Fig. 3, *A* and *C*, *lanes 7*) and wild-type HEK293 cells (Fig. 3*A*, *lane 8*), used as negative controls, did not react with the anti-NOX5 Ab. NOX5-transfected HEK293 cells, a positive control for the specificity of the NOX5 Ab, produced a band of the same size as that detected in HCs (Fig. 3*A*, *lane 9*).

We then used RT-PCR and found that some of the HC samples (Fig. 3*B*), but none of those prepared from CLL ($n = 6$) or MZL ($n = 1$) or from normal peripheral blood B cells ($n = 3$) (Fig. 3*D*), generated the 433-bp band predicted to be produced by the primers used for the NOX5 PCR. As a positive control, cDNA prepared from NOX5-transfected HEK293 cells was used (Fig. 3*D*, *lane 7*). The quality of the mRNA preparations was satisfactory as judged by the expression of *gapdh* or *β-actin* (Fig. 3, *B* and *D*). In addition, the fidelity of the transcription of *nox5* was confirmed by sequencing a subclonal PCR product derived from cells of case 4 in Fig. 3*B*, and this was identical to the sequence within human NOX5 cDNA from nt 1939–2371 (GenBank accession No. AF325190).

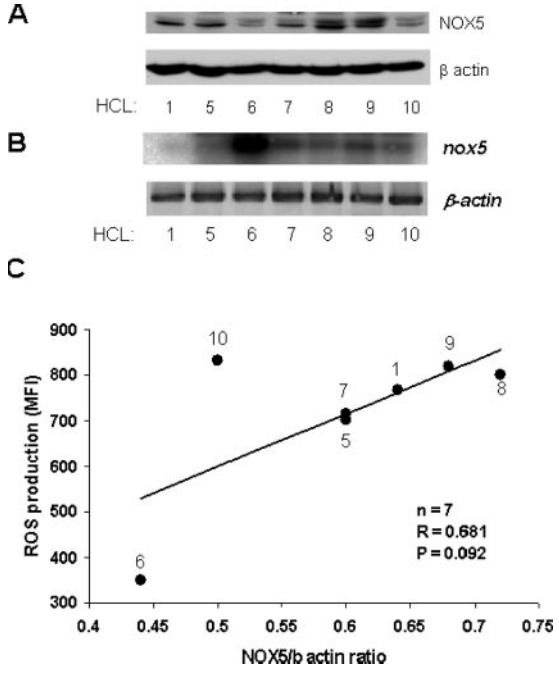

FIGURE 4. All HC clones express NOX5, and oxidant production correlates with NOX5 protein levels. *A*, A total of 10^6 cells from seven HCL cases were lysed, and the lysates were analyzed by Western blotting for NOX5 and β-actin. The intensities of the bands were measured by densitometry and NOX5 to β-actin ratios were calculated. *B*, nox5 PCR products from cDNA of seven HCL cases detected by Southern hybridization using a ^{32}P-labeled probe (*upper panel*). Negative images of β-actin amplified by PCR from the same cDNA samples are shown in the *lower panel. C*, ROS production (measured as in Fig. 1) by the same cases (10^6 cells/ml) shown in *A* and *B* in relation to NOX5 protein levels expressed as NOX5 to β-actin ratios. Pearson's linear correlation analysis was used to calculate the relationship between ROS production and NOX5 expression.

To verify whether HC purification had an effect on the expression of NOX5, we also used HCs without depletion of T cells and monocytes. Results in Fig. 3*E* show that this had no effect on expression of either protein or message for NOX5.

In contrast to the consistent, although variable, levels of NOX5 protein in HCs, the expression of its mRNA when measured by RT-PCR ranged from nondetectable to strongly positive (Fig. 3*B*). However, when a more sensitive Southern blotting hybridization method was used (see *Materials and Methods*), *nox5* expression was detected in all seven HCL cases tested (Fig. 4*B*).

There was no clear correlation between NOX5 message and the variably expressed NOX5 protein. However, when the protein levels (Fig. 4*A*) were correlated with ROS production, a Pearson's linear correlation analysis showed a trend toward a positive correlation ($p = 0.09$; n = 7; Fig. 4*C*). Also, when the rates of O_2^- production by the cells of the two cases shown in Fig. 2 were examined, the rate of ROS production was 3-fold higher in HCL2, the cells of which contained more NOX5 protein (data not shown).

Because NOX5 expression has been previously demonstrated in lymphoid tissue but not in cells in the circulation (11), we believe the present data constitute the first demonstration of NOX5 in circulating, albeit malignant, B cells.

The presence of NOX5 in HCs and its absence in the other examined B cell types suggest that NOX5 expression in HCs could be a consequence of some specific activation features of these cells that are absent from the other B cell types. Therefore, we next examined whether NOX5 expression could be a consequence of

some specific intrinsic or extrinsic stimuli relevant for the phenotype of HCs (1, 23).

PKC activation and certain relevant HC interactions with the tissue microenvironment are not involved in the induction of NOX5

Because HCs contain active PKC (5) and because treatment of CLL cells with phorbol esters induces some phenotypic features found in HCs (24, 25), we next examined whether activation of PKCs in CLL cells induces NOX5 expression. In fact, exposure of CLL cells to PMA and bryostatin (10 nM each) for 24 h did not induce NOX5 in these cells (data not shown).

The reported presence of NOX5 in lymphoid tissues, but not in circulating cells (10, 11), suggests that cell interactions with the tissue microenvironment may be responsible for the induction of this enzyme. Within tissues, HCs are known to interact strongly with fibronectin and vitronectin (16) and also respond to GM-CSF (26), a cytokine that induces expression of gp91^{phox} in human myeloblastic leukemia cells (27). Therefore, we cultured HCs for up to 48 h on a nonadherent, polyHEMA-coated surface or on plates coated with equal amounts of fibronectin and vitronectin (20 μg/ml each), in the absence or presence of 0.1 ng/ml GM-CSF. At 0, 24, and 48 h of culture, samples were analyzed by RT-PCR and Western blotting for NOX5 expression. Results showed that this in vitro stimulation had little or no effect on either NOX5 mRNA or protein expression in HCs (data not shown). Therefore, the stimulus for the specific expression of NOX5 by HCs remains unclear.

Because HCs show pronounced protein tyrosine phosphorylation and because ROS are known to inactivate PTPs (12–14), we next examined the effect of oxidant production on the activity of these enzymes in HCs.

An NADPH oxidase inhibitor (DPI) increases the activity of the PTP SHP-1 in HCs

The treatment of HCs with DPI caused a significant increase in the phosphatase activity measured in whole-cell lysates of either purified (Fig. 5*A*) or nonpurified cells. This clearly demonstrated inhibition by ROS of the activity of PTPs in HCs. We then assessed the contribution of immunoprecipitated PTPs, SHP-1, SHP-2, and PTP-1B to overall phosphatase activity, and examined the effect of cell treatment with DPI on the activities of these enzymes.

In HCs, protein tyrosine phosphorylation signals closely resemble those emanating from the BCR (5). Because these signals are negatively regulated by SHP-1, we focused on this enzyme but also examined the activities of SHP-2 and PTP-1B to establish whether or not ROS production by NOX5 indiscriminantly inhibits all three phosphatases. DPI treatment caused a significant increase in SHP-1 activity, but had no effect on the activities of SHP-2 or PTB-1B (Fig. 5*C*). The immunoprecipitation of phosphatases was confirmed by Western blotting (Fig. 5*D*). As expected, protein tyrosine phosphorylation was reduced in DPI-treated HCs (*Fig. 5B*), demonstrating the impact of the increased SHP-1 activity on the protein tyrosine phosphorylation signals in DPI-treated cells.

In B cells, SHP-1 becomes activated by binding to phosphorylated ITIMs (ITIM motifs) on CD22 (28) and then down-regulates signals required for Ca^{2+} mobilization after BCR cross-linking (29). Therefore, it seemed important to examine the phosphorylation state of CD22 in HCs, together with the association of SHP-1 with this protein and possibly also with NOX5.

In HCs, SHP-1 is recruited by tyrosine phosphorylated CD22 and is in the same cell compartment as NOX5

To investigate whether CD22 is phosphorylated in HCs, the protein was immunoprecipitated from cell lysates and analyzed by Western blotting using an anti-phosphotyrosine Ab. Results showed that CD22 is indeed constitutively tyrosine phosphorylated in HCs (Fig. 6*A*), most likely by a Src family kinase in its ITIM motifs. Reprobing of the blotted proteins with anti-SHP-1 Ab demonstrated that SHP-1 coimmunoprecipitates with CD22 (Fig. 6*B*). Thus, it is likely that, in HCs, phosphorylated CD22 recruits SHP-1 to the membrane where the enzyme normally dephosphorylates tyrosine phosphorylated proteins. Because, on the contrary, tyrosine phosphorylation is increased in HCs, it seemed possible that the SHP-1 recruited to the membrane by CD22 was largely inactivated by ROS produced by NOX5 present in the membrane in close proximity.

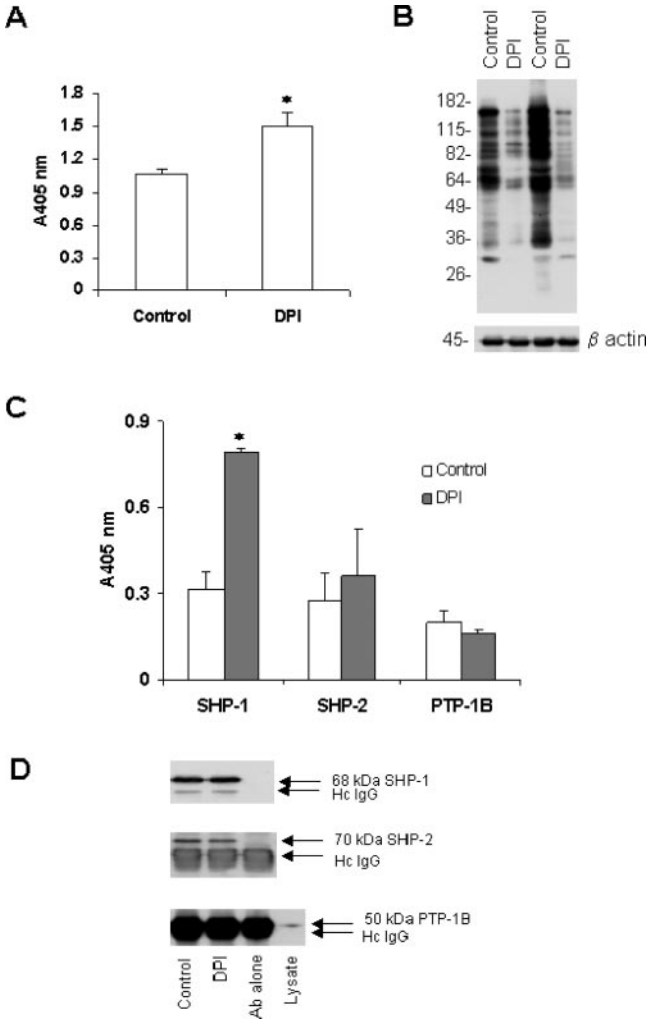

FIGURE 5. DPI treatment increases PTP activity in HCs. *A*, PTP activity of lysates from controls and DPI (5 μM)-treated HCs. PTP activity was detected using pNPP as substrate. Results are means ± SD of duplicate measurements involving cells from four different patients (*, $p = 0.0075$; paired-sample Student's *t* test). *B*, The effect of DPI (5 μM) on total protein tyrosine phosphorylation in two HCL cases. β-Actin levels are shown as equal loading controls. *C*, PTP activity of immunoprecipitated SHP-1, SHP-2, and PTP-1B from HC lysates in which cells were untreated or treated with 5 μM DPI for 1 h. Results are shown as means ± SD of three independent experiments with cells from three different HCL patients (*, $p = 0.0021$; paired-sample Student's *t* test). *D*, The levels of immunoprecipitated SHP-1, SHP-2, and PTP-1B by Western blotting (representative example of three independent experiments involving three patients). Because the size of PTP-1B coincides with that of the Ab (Hc, H chain) used for immunoprecipitation, PTP-1B in the whole cell lysate is also shown.

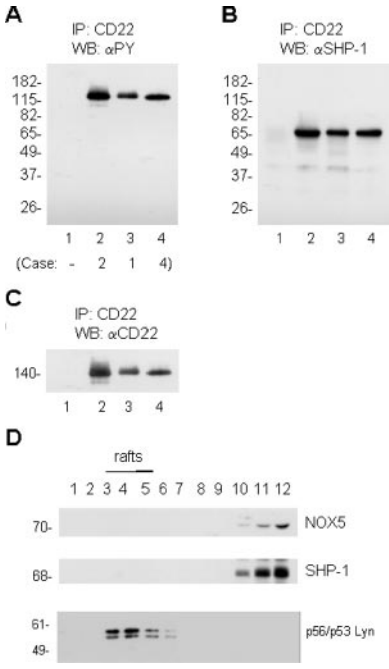

FIGURE 6. SHP-1 coprecipitates with tyrosine-phosphorylated CD22 and is found in the same membrane fractions as NOX5. CD22 was immunoprecipitated with an anti-CD22 Ab from cells of three HCL cases (10^7 cells) lysed in 1% Nonidet P-40 lysis buffer containing 50 mM Tris-HCl (pH 8), 150 mM NaCl, 2 mM EDTA, 50 mM NaF, 1 mM Na_3VO_4, 1 mM PMSF, 1 μg/ml leupeptin, and 1 μg/ml aprotinin. The immunoprecipitates were subjected to SDS-PAGE and Western blotting with anti-phosphotyrosine Ab (*A*). Blots were reprobed with anti-SHP-1 (*B*) and anti-CD22 (*C*) Abs. *Lane 1*, Mouse IgG1; *lanes 2–4*, CD22 immunoprecipitates from cells of three patients. *D*, Immunoblots of NOX5, SHP-1, and Lyn (a marker in B cells of membrane lipid rafts) in membrane subcellular fractions (5 μg) prepared as described in *Materials and Methods*. Similar results were obtained with cells from two other HCL cases.

To examine whether this is so, we prepared membrane lipid raft and nonraft fractions and analyzed each for NOX5 and SHP-1 by Western blotting. This showed that NOX5 and SHP-1 were absent from membrane lipid rafts, but were both present in the same nonraft membrane fractions (Fig. 6*D*).

Altogether, our study demonstrates that NOX5 in HCs has an important role in the generation of ROS that participate in the regulation of the constitutive activation of these cells.

Discussion

The present work was initially undertaken to determine whether the active Rac-1 and PKCs in HCs are involved in oxidant production.

We found that oxidant production in HCs was independent of these two proteins and involved a plasma membrane-associated enzyme that required only Ca^{2+} for its activity. This led to the characterization of the oxidase as NOX5, an enzyme not previously demonstrated in circulating lymphocytes (11). In contrast to HCs, the malignant cells of CLL, MZL, and MCL, as well as normal peripheral blood B cells contained either no or only trace amounts of NOX5 protein or message.

NOX5 is an NADPH oxidase that, in contrast to the oxidase of phagocytic leukocytes, does not require cytosolic components including Rac1 because its regulatory and catalytic modules are combined within one protein (9). Therefore, our demonstration of a constitutively active NADPH oxidase in HCs can be explained by the presence of NOX5 activated by the previously demonstrated high levels of cytosolic Ca^{2+} in these cells (2).

We also explored some of the mechanisms that could be responsible for the selective expression of NOX5 by HCs. The reported presence of NOX5 in lymphoid tissues (10) suggested that NOX5 expression might be dependent on stimuli originating from the tissue microenvironment. It is known that HCs accumulate in the spleen and bone marrow where they, respectively, interact with vitronectin and fibronectin (23). Therefore, we cultured HCs on these adhesive ligands in the presence or absence of GM-CSF, a cytokine known to enhance HC adhesion (26) and to induce $gp91^{phox}$ in malignant myeloid cells (27). However, this did not increase NOX5 expression by HCs. Also, stimulation of CLL cells with PMA—a treatment reported to induce a number of HC-like features (24, 25)—did not stimulate NOX5 expression in these cells. Therefore, whether the expression of NOX5 by HCs is a feature of intrinsic or extrinsic activation or reflects the particular as-yet-unknown origin or the differentiation stage of these cells remains unclear.

We next examined the importance of NOX5-derived oxidants for the constitutive activation of HCs. HCs show constitutively active protein tyrosine kinases (PTKs) (3, 5) and these enzymes are opposed by PTPs (12–14). Because ROS are known to inhibit PTPs, we measured the activity of these enzymes in HCs before and after inhibition of oxidant production. We found that this inhibition potentiated the activity of PTPs, especially that of SHP-1. SHP-1 is an SH2 domain-containing tyrosine phosphatase predominantly expressed in hemopoietic cells where it dephosphorylates proteins phosphorylated by PTKs. SHP-1 is recruited to the signaling complex formed after Ag-receptor (BCR) ligation by binding to tyrosine phosphorylated ITIM motifs on CD22 (29). We demonstrated that CD22 is indeed tyrosine phosphorylated in HCs and that SHP-1 coimmunoprecipitates with this protein. Moreover, using subcellular fractionation, we found that SHP-1 and NOX5 are present in the same nonraft membrane compartment where they may be closely associated. The notion that SHP-1 specifically coassociates with NOX5 is supported by the finding that inhibition of oxidase production by DPI selectively increased the activity of SHP-1, but not SHP-2 or PTP-1B.

In conclusion, the present study demonstrates for the first time that circulating HCs express NOX5. Moreover, we demonstrate that NOX5 is closely associated at the cell membrane with CD22-recruited SHP-1 and that NOX5-generated oxidants inhibit this phosphatase. Therefore, NOX5 appears to play an important role in the regulation of constitutive phosphorylation signals in HCs.

Acknowledgments

We are grateful to Prof. Alan Hall (University College London) for the gift of the plasmid clone pGEX-PAK.

Disclosures

The authors have no financial conflict of interest.

References

1. Cawley, J. C., M. Zuzel, and F. Caligaris-Cappio. 2000. Biology of hairy cells. In *Advances in Blood Disorders*. M. S. Tallman, and A. Polliack, eds. Harwood Academic Press, Amsterdam, Holland, p. 9–18.
2. Genot, E., G. Bismuth, L. Degos, F. Sigaux, and J. Wietzerbin. 1992. Interferon-α downregulates the abnormal intracytoplasmic free calcium concentration of tumor cells in hairy cell leukemia. *Blood* 80: 2060–2065.
3. Linch, S. A., J. S. Brugge, F. Fromovitz, L. Glantz, P. Wang, R. Caruso, and M. V. Viola. 1993. Increased expression of the src proto-oncogene in hairy-cell leukemia and a subgroup of B-cell lymphomas. *Leukemia* 7: 1416–1422.
4. Zhang, X., T. Machii, I. Matsumura, S. Ezoe, A. Kawasaki, H. Tanaka, S. Ueda, H. Sugahara, H. Shibayama, M. Mizuki, and Y. Kanakura. 2003. Constitutively activated Rho guanosine triphosphatases regulate the growth and morphology of hairy cells. *Int. J. Hematol.* 77: 263–273.

5. Kamiguti, A. S., R. J. Harris, J. R. Slupsky, P. K. Baker, J. C. Cawley, and M. Zuzel. 2003. Regulation of hairy-cell survival through constitutive activation of mitogen-activated protein kinase pathways. *Oncogene* 22: 2272–2284.
6. Bokoch, G. M., and U. G. Knaus. 2003. NADPH oxidases: not just for leukocytes anymore. *TRENDS Biochem. Sci.* 28: 502–508.
7. Lassegue, B., and R. E. Clempus. 2003. Vascular NAD(P)H oxidases: specific features, expression and regulation. *Am. J. Physiol.* 285: R277–R297.
8. Banfi, B., F. Tirone, I. Durussel, J. Knisz, P. Moskwa, G. Z. Molnar, K.-H. Krause, and J. A. Cox. 2004. Mechanism of Ca^{2+} activation of the NADPH oxidase 5 (NOX5). *J. Biol. Chem.* 279: 18583–18591.
9. Cheng, G., Z. Cao, X. Xu, E. G. van Meir, and J. D. Lambeth. 2001. Homologs of $gp91^{phox}$: cloning and tissue expression of Nox3, Nox4 and Nox5. *Gene* 269: 131–140.
10. Banfi, B., G. Z. Molnar, A. Maturana, K. Steger, B. Hegedus, N. Demaurex, and K.-H. Krause. 2001. A Ca^{2+}-activated NADPH oxidase in testis, spleen and lymph nodes. *J. Biol. Chem.* 276: 37594–37601.
11. Krause, K.-H. 2004. Tissue distribution and putative physiological function of NOX family NADPH oxidases. *Jpn. J. Infect. Dis.* 57: 28–29.
12. Zhao, Z., Z. Tan, C. D. Diltz, M. You, and E. H. Fischer. 1996. Activation of mitogen-activated protein (MAP) kinase pathway by pervanadate, a potent inhibitor of tyrosine phosphatases. *J. Biol. Chem.* 271: 22251–22255.
13. Denu, J. M., and K. G. Tanner. 1998. Specific and reversible inactivation of protein tyrosine phosphatases by hydrogen peroxide: evidence for a sulfenic acid intermediate and implications for redox regulation. *Biochemistry* 37: 5633–5642.
14. Barrett, W. C., J. P. DeGnore, Y.-F. Keng, Z.-Y. Zhang, M. B. Yim, and P. B. Chock. 1999. Roles of superoxide radical anion in signal transduction mediated by reversible regulation of protein-tyrosine phosphatase 1B. *J. Biol. Chem.* 274: 34543–34546.
15. Davey, P. C., M. Zuzel, A. S. Kamiguti, J. A. Hunt, and, K. A. Aziz. 2000. Activation-dependent proteolytic degradation of polymorphonuclear cells. *Br. J. Haematol.* 111: 934–942.
16. Burthem, J., P. K. Baker, J. A. Hunt, and J. C. Cawley. 1994. Hairy cell interactions with extracellular matrix: expression of specific integrin receptors and their role in cell's response to specific adhesive proteins. *Blood* 84: 873–882.
17. Benard V., B. P. Bohl, and G. M. Bokock. 1999. Characterization of rac and cdc42 activation in chemoattractant-stimulated human neutrophils using a novel assay for active GTPases. *J. Biol. Chem.* 274: 13198–13204.
18. Shpungin, S., I. Dotan, A. Abo, and E. Pick. 1989. Activation of the superoxide forming NADPH oxidase in a cell-free system by sodium dodecyl sulphate. *J. Biol. Chem.* 264: 9195–9203.
19. Oliferenko, S., K. Paiha, T. Harder, V. Gerke, C. Schwarzler, H. Schwartz, H. Beug, U. Gunthert, and L. A. Huber. 1999. Analysis of CD44-containing lipid rafts: recruitment of annexin II and stabilization by the actin cytoskeleton. *J. Cell Biol.* 146: 843–854.
20. Sergeant S., and L. C. McPhail. 1997. Opsonized zymosan stimulates the redistribution of protein kinase C isoforms in human neutrophils. *J. Immunol*. 159: 2877–2885.
21. Bokoch, G.M., and B. A. Diebold. 2002. Current models for NADPH oxidase regulation by Rac GTPase. *Blood* 100: 2692–2696.
22. Genot, E.M., K. E. Meier, K. A. Licciardi, N. G. Ahn, C. H. Uittenbogaart, J. Wietzerbin, E. A. Clark, and M. A. Valentine. 1993. Phosphorylation of CD20 in cells from a hairy cell leukemia cell line: evidence for involvement of calcium/calmodulin-dependent protein kinase II. *J. Immunol.* 151: 71–82.
23. Burthem J., and J. C. Cawley. 1996. *Hairy-Cell Leukaemia*. Springer-Verlag, London.
24. Caligaris-Cappio, F., G. Pizzoto, M. Chilosi, L. Bergui, G. Semenzato, L. Tesio, L. Morittu, F. Malavasi, M. Gobbi, and R. Schwarting. 1985. Phorbol ester induces abnormal chronic lymphatic leukaemia cells to express features of hairy-cell leukaemia. *Blood* 66: 1035–1042.
25. Visser, L., and S. Poppema. 1990. Induction of B-cell chronic lymphocytic leukaemia and hairy cell leukaemia-like phenotypes by phorbol ester treatment of normal peripheral blood B-cells. *Brit. J. Haematol.* 75: 359–365.
26. Till, K. J., J. Burthem, A. Lopez, and J. C. Cawley. 1996. Granulocyte-macrophage colony-stimulating factor receptor: stage-specific expression and function on late B cells. *Blood* 88: 479–486.
27. Shimizu, T., R. Kodama, S. Tsunawaki, and K. Takeda. 2002. GM-CSF induces expression of $gp91^{phox}$ and stimulates retinoic acid-induced $p47^{phox}$ expression in human myeloblastic leukaemia cells. *Eur. J. Haematol.* 68: 382–388.
28. Blasioli, J., S. Paust, and M. L. Thomas. 1999. Definition of the sites of interaction between the protein tyrosine phosphatase SHP-1 and CD22. *J. Biol. Chem.* 274: 2303–2307.
29. Nitschke L., R. Carsetti, B. Ocker, G. Kohler, and M. C. Lamers. 1997. CD22 is a negative regulator of B-cell receptor signalling. *Curr. Biol.* 7: 133–143.